

PAPER REF: 5563

## STUDY OF CFRP-PEEK BONE PLATES: TEST AND FEM ANALYSIS

M. Castro<sup>1</sup>, P. Aguiar<sup>2</sup>, A. Barreiro<sup>3</sup>, J.D. Barreiro<sup>3</sup>, E. Casarejos<sup>1(\*)</sup>, A. Gonzalez<sup>3</sup>, A. Iglesias<sup>1</sup>,  
P. Izquierdo<sup>1</sup>, M.C. Pérez<sup>2</sup>, A. Segade<sup>1</sup>, M. Vila<sup>3</sup>, J.A. Vilán<sup>1</sup>, P. Yañez<sup>1</sup>

<sup>1</sup>Escuela de Ingeniería Industrial, Universidade de Vigo, E-36310 Vigo, Spain

<sup>2</sup>Fundación Ramón Domínguez, CHUS, E-15706 Santiago de Compostela, Spain

<sup>3</sup>HVU Rof Codina, Dpto. Ciencias Clínicas Veterinarias, Univ. de Santiago de Compostela, 27002 Lugo, Spain

(\*)Email: e.casarejos@uvigo.es

### ABSTRACT

This paper describes the mechanical characterization of plates made of peek reinforced with (long) carbon fibres (CFR-PEEK), based in commercial pre-pregs. We have produced and measured samples to serve as reference to a calculation model. Using a finite element model reference program dedicated to composites (ANSYS-ACP) we have validated the results of bending tests required to study the bone plates. The aim was to test an analysis model that can be used as guide to re-define and optimize the bone plates for animals (rabbits), for future in-vivo tests.

**Keywords:** carbon fibre reinforced peek, peek, CFRP, composites, ANSYS ACP, bone plates.

### INTRODUCTION

Poly(aryl-ether-ether-ketone) (PEEK) is a polymer with outstanding technical properties, approved for human use in long-term implants, and often used in spine implants. The identification of peek reinforced with carbon fibre (CFR-PEEK) as a suited material for internal fracture fixation (bones plates) is traced back to 1990s, and despite the early successful results of semi-rigid plates (Tayton, 1982) (Ali, 1990), the interest has been mostly restricted to research. The limited results are reviewed by (Scholz, 2011) and (Kurz, 2007)<sup>1</sup>. At this time there is not yet widespread clinical reports related to the use of CFR-PEEK for bone plates. This situation is due both to the discussion about the use of semi-rigid plates and a manufacturing limitation.

The interest for less rigid plates is linked to the long standing discussion about the effects of stress shielding in the bone healing process, initiated in the 1980s. Later works show that the bending stiffness of the whole fixation (plate, bone and screws) would be studied together. Not only the material of the plate played a role, but namely its moment of inertia, thus the relative position, plate design and fastening procedure (Cordey, 2000) (Gautier, 2000). The interest in CFR-PEEK is today taken from other points of view. On the one side the radiolucent properties for applying high-quality imaging methods for the survey of trauma patients. On the other side, the demand by surgeons of widening the treatment options to deal with an increasing number of patients with risk factors for different complications.

---

<sup>1</sup> The author mentions a key company that sold about 1000 CFR-epoxy plates in the period 1982-2007 in the USA, while about 600000 fixation procedures of long bones were done just in 2004 in that country.

There exists a clear limitation for the deployment of CFRP plates linked to the manufacturing procedures of complex composites. Some authors have developed sophisticated knitted and braided CFR-PEEK fibres to increase the properties of laminated and unidirectional (fibre oriented) plates, and studied the plate design based in a progressive failure analysis (Huang, 2001, 2005) (Fujihara, 2003, 2004). Beyond research, only two companies known to the authors produce and market extruded long-fibre CFR-PEEK plates and screws (Icotec AG, Switzerland) (CarboFix Orthopedics Ltd., Israel), linked to a unique company providing medical grade CFR-PEEK suitable for long-term implantation (Invibio Limited, UK).

CFRP-peek pre-pregs are available in the market only recently, opening more effective procedures to manufacture high-quality plates. For the tests we used the pre-preg product TPUD manufactured by Toho Tenax Europe GmbH (Germany). Our group started a program to use CFRP-PEEK pre-pregs with the ultimate goal of testing bone plates with rabbits.

Different work lines are needed to obtain data in order to produce a suitable and feasible plate prior to any test in-vivo. Therefore we started with basic studies of the material to produce first a reliable model and later evaluate the design options of the plates. If probed reliable, this virtual test-bench can make effective the feedback procedure for re-designing the plates, plan more functional tests, until a final stage of in-vivo studies.

## MATERIAL CHARACTERIZATION

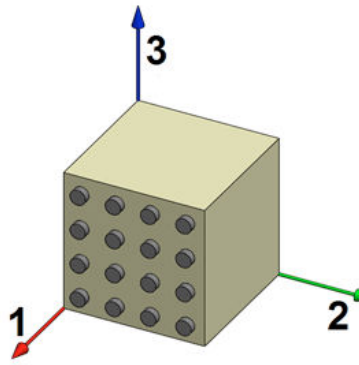
The model of the plate relies in one side in a finite element model (FEM) describing the composite behaviour, and in the other side in the proper characterization of the properties of the material, which is always a challenge with composites. We have paid a special attention into the collection of data used to properly define our CFR-PEEK plates. We used experimental data whenever provided by the manufacturer and dedicated models of micromechanics of composites for derived parameters.

For the PEEK matrix, a homogenous and isotropic material, the properties are well established, and only minor differences arise from high-quality PEEK providers.

The entangling of the properties of each basic material, the homogeneous matrix and the long fibre, into the properties of the composite depends many times on the ratio of both (rule of mixtures). This ratio can be difficult to define in traditional lamination processes. However, pre-pregs have a well-defined ratio, and the processing into final shapes does not change significantly that value. In our case the ratio of PEEK matrix ( $k^m$ ) is quoted in the technical specifications as 34% in weight. The manufacturer also quotes the ratio of fibre  $k^f = 60\%$  in volume (Gilliot, 2012). There are no references for possible (micro) volumes of porosity in the impregnation of the fibres, although the manufacturer claims that the high degree of peek impregnation is largely reflected in the CFR-PEEK properties achieved.

In the following we resume all the material parameters that we have defined and used for our calculations. The values are resumed in Table.1 for both PEEK and the CFR-PEEK used in our work. We used a notation based in the axis labels (1, fibre orientation and longitudinal plate axis; 2, transverse axis, corresponding to the plate width; 3, transverse axis, being the ply stacking direction) as described in the scheme of Table.1, as well as labels  $f$  and  $m$  to refer to fibre and matrix, respectively.

Table 1 - Material properties used in the calculations. The axis and planes for the orientations are those of the figure in the left. Labels (+) and (-) are used to indicate tensile or compression stress. The values for PEEK are those quoted for PEEK OPTIMA (Invibio Limited, UK). The values for the CFR-PEEK are either provided by the fabricant, or obtained with reference composite models. See text for details.



	CFR-PEEK	PEEK	
Elastic modulus $E_1$	142	3.7	[GPa]
$E_2 = E_3$	5	3.7	[GPa]
Shear modulus $G_{12} = G_{13}$	4.6	1.3	[GPa]
$G_{23}$	1.9	1.3	[GPa]
Strength $S_{1+} / S_{1-}$	2450 / 1545	97 / 118	[MPa]
$S_{2+} = S_{3+} / S_{2-} = S_{3-}$	88 / 88	97 / 118	[MPa]
Shear strength $S_{12} = S_{13}$	43.8	53	[MPa]
$S_{23}$	46.8	53	[MPa]
Poisson's coeff. $V_{12} = V_{13}$	0.26	0.4	
$V_{23}$	0.32	0.4	

## Elastic modulus

**Longitudinal ( $E_1$ ).** This value is provided by the manufacturer,  $E_1 = 142$  GPa (DIN EN 2561 Type A). It corresponds closely with the value of the carbon fibre type used in the pre-preg (TENAX HTS45,  $E_1^f = 240$  GPa) and weighted by the content of fibre in the composite, using the rule of mixtures ( $E_1 = k^f \cdot E_1^f + k^m \cdot E^m$ ).

**Transverse ( $E_2 = E_3$ ).** To define this parameter, we used the micromechanics equations for composites of Hopkins-Chamis (Hopkins, 1985). The authors provide a general form to relate composite properties from the same parameters of the fibre and matrix, and the ratio of fibre content:

$$E_2 = E^m \left[ (1 - \sqrt{K^f}) + \frac{\sqrt{K^f}}{1 - \sqrt{K^f} \left( 1 - E^m / E_2^f \right)} \right] \quad (1)$$

being  $E^m$  the modulus of the matrix (isotropic), and  $E_2^f$  the transverse modulus of the fibre. It is known that the ratio  $E^m / E_2^f$  is about 0.6 (Miyagawa, 2006), as a conservative option. Therefore we obtain  $E_2 = E_3 = 5.0$  GPa.

## Shear modulus

Following the same formulation of Hopkins-Chamis and with the same format as Eq.(1), we can define the shear moduli of the composite from the shear moduli of matrix and fibre.

**In-plane ( $G_{12} = G_{13}$ ).** We need to define the shear modulus  $G_{12}^f$  of the fibre. That can be obtained from the general relationship for orthotropic materials, relating the elastic and shear moduli and Poisson's ratio:

$$G_{12}^f = \frac{E_1^f}{2(1 + \nu_{21}^f)} \quad (2)$$

The value of  $\nu_{21}^f$  (Poisson's coefficient) is expected to be rather low compared to unity. It can be evaluated from the reciprocity relation for plane elasticity given by  $E_1^f \nu_{21}^f = E_2^f \nu_{12}^f$  for  $\nu$  being the Poisson's coefficients.

Considering  $E_1^f = 240$  GPa, the ratio used before for  $E^m/E_2^f$ , and the typical value of  $\nu_{12}^f = 0.2$  (Chamis, 1983), it results  $\nu_{21}^f = 0.008$ . Therefore,  $G_{12}^f = 116.5$  GPa, and finally we obtain

$$G_{12} = G_{13} = 4.6 \text{ GPa.}$$

**Inter-lamina ( $G_{23}$ ).** Considering the equivalent relationship as in Eq.(2), and typical values  $\nu_{23}^f = 0.25$  (Chamis, 1983), we get  $G_{23}^f = 2.5$  GPa, thus  $G_{23} = 1.9$  GPa.

### Poisson coefficients

**In-plane** ( $\nu_{12} = \nu_{13}$ ). Using the rule of mixtures, and considering again  $\nu_{12}^f = 0.2$ , we obtain  $\nu_{12} = \nu_{13} = 0.26$ .

**Inter-lamina** ( $\nu_{23}$ ). This value can be obtained from general relations of composite micromechanics (Chamis, 1983)

$$G_{23} = \frac{E_2}{2(1+\nu_{23})} \quad (3)$$

and from the derived results,  $\nu_{23} = 0.32$ .

### Strength

**Longitudinal.** Given by the fabricant:

Tensile  $S_1^+ = 2450$  MPa (DIN EN 2561 Type A).

Compression  $S_1^- = 1545$  MPa (EN 2580 Type A3).

### Transverse

Tensile  $S_2^+ = S_3^+ = 88$  MPa (DIN EN 2597 Type B), given by the fabricant. This value, for a UD laminate, is ruled mostly by the properties of the matrix. However the quoted value is rather close to that of the matrix itself  $S^{m+}$ , overpassing the rule of mixture. This gives also an idea of the quality of the PEEK impregnation of the fibres achieved in this product. This value is not critical for a bending test. However, it will be important in the design of a plate, since it defines the behaviour of the walls around the drills for screws.

Compression  $S_2^- = S_3^- = 88$  MPa. This value is typically higher than  $S_2^+$ . We use the same value as a conservative option. The value of  $S_3^-$  is very important in order to describe the possible crushing of the plate by the loading rollers of the test.

### Shear strength

The shear strengths can be obtained from relations of composite micromechanics (Chamis, 1984), based in matrix and fibre shear values, and mixture ratios. The results follow straightforward by using as input parameters  $k_f$ ,  $G^m$ ,  $G_{12}^f$ ,  $S^{m+}$ ,  $G_{23}^f$ , and results

(intra-laminar shear)  $S_{12} = 43,8$  MPa

(inter-lamina shears)  $S_{13} = 43,8$  MPa ;  $S_{23} = 46,8$  MPa.

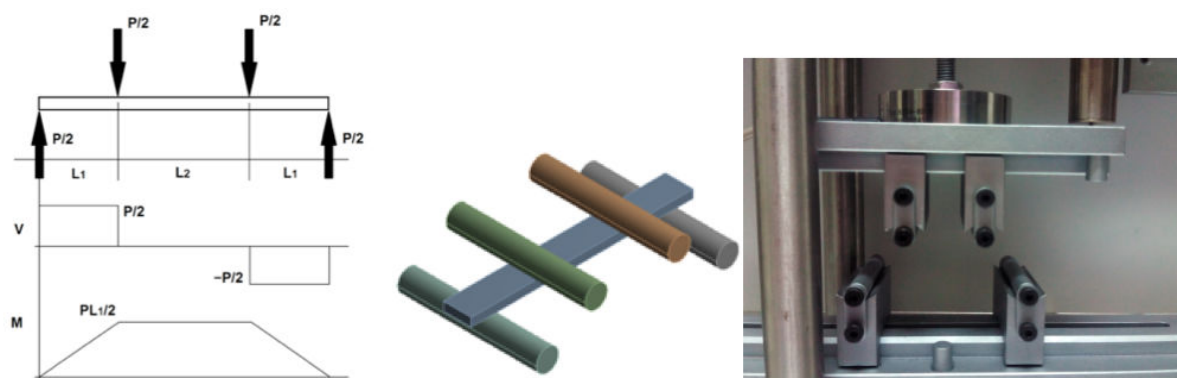


Fig. 1 - The four-point bending test is made by the application of loads with loading rollers, transverse to the longitudinal axis of the coupons, as shown in the left and central schemes. The distribution of bending moment ( $M$ ) is constant in between the rods, and it can be given straightforward from the load and geometry values. In the right, a picture of part of the test bench made for the measurements. The load cell on top is visible.

## BENDING TEST

### Coupon preparation

In order to test the material in a bending bench, we have prepared coupons of 10 mm width, 80 mm length, with pre-preg plies 0.13 mm thick, making a stack of 23 layers. The fibre direction is that of the longitudinal axis of the coupons. For processing the pre-preg we loaded the mould with 30 bars previous to fastening, heated in a furnace for 1.5 h hours at 400° C, and cooling slowly within the furnace. The resulting coupons show compact and solid surfaces, and a stack thickness constant within 0,02 mm.

### Bending test bench

In order to follow the standards for bending test dedicated to bone plates, according to ASTM F382 and ISO 9585, we designed and built a dedicated bench for a four-point bending test. The main purpose of the design was to accommodate the sizes and load ranges of our program, dedicated to CFR-PEEK plates for rabbits. The operation is manual, with a threatened rod, and we only have to consider a limited turn speed to achieve a reasonable (1 mm/min) deflection rate. The readout of a load cell and a displacement gauge (both from Burster praezisionsmesstechnik gmbh & co kg, Germany), gives a straight measure of the bending parameters. The calibration of load and displacement gauges give values with an uncertainty below 3% in the range of our tests. The bench can accommodate plates ranging from 50 up to 200 mm length, 20 mm width, and loads up to 10 kN.

Both mentioned standards refer to the geometry positioning of bone plates, considering the plate lengths and holes, as well as recommending loading roller diameters related to plate thicknesses. However, there are no standards for bending tests of materials, although are commonly used for research purposes. Some discussions of the methodology and FEM calculations for thin composite laminates are found in (deBaere, 2009).

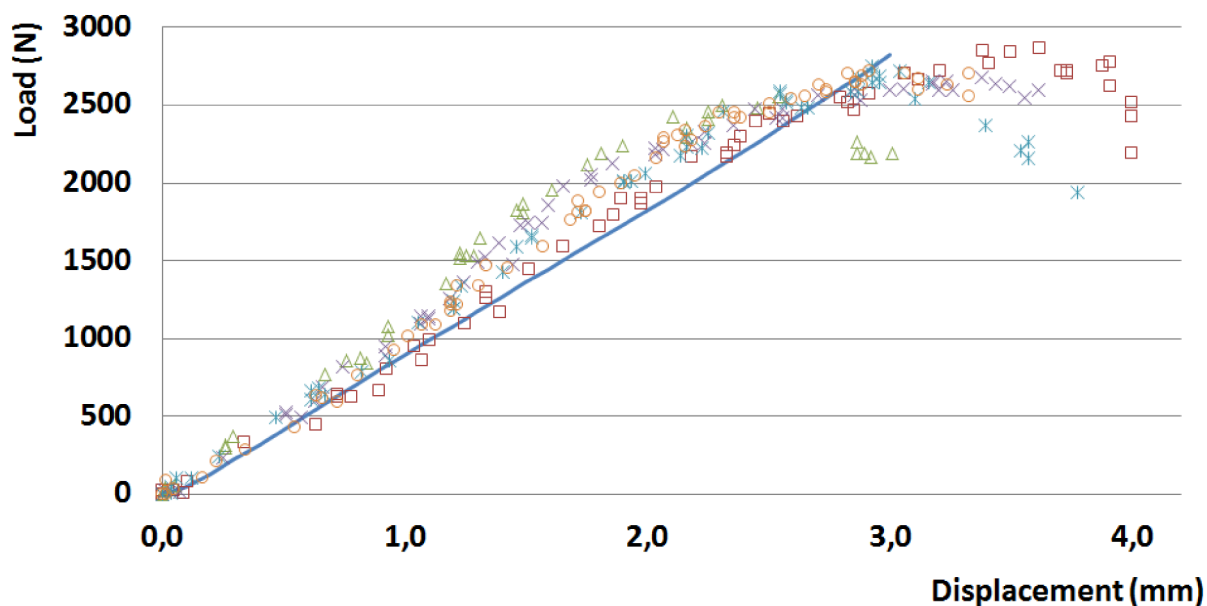


Fig. 2 - Bending measurement of five coupons made as a stack of 23 plies of mono-directional CFR-PEEK prepreg TPCU (Toho-Tenax, Germany). The load is applied in a four-point bench. The displacement corresponds to the mid-span of the coupons. A clear linear trend follows up to 2 mm displacement. After that point, cracks are observed, and the data bends till total failure happens. The line correspond to the results of the FEM calculation done, based in the material characterization described in this work. See text for details.

In a four-point bending test, see Fig.1, the bending moment applied is well defined between the loading rollers, and the bending stiffness of the plate is defined straightforward, according to the linear bending theory from the mid-span displacement and the geometry. It is worth to note that we are only interested now in a quasi-static bending test.

In Fig.2 we show the result of measuring a batch of five equal coupons, as the load and mid-span displacement during the test. The linear range is clearly visible. About a mid-span displacement of 2 mm and a load of 2.1 kN, the coupons start breaking, changing clearly the slope of the trend. We check that the linearity of the data changes notably if the range is extended beyond 2 mm. For values close to 3 mm, we could also observe the initial macroscopic cracks, and the total failure of the plate. The behaviour after the initial cracks is more erratic due to the different propagation ways that may happen. Since we are only interested in the stress distribution up to the first failure, our data, observed with spreads of load and displacement typically below 10%, give us a consistent picture.

## FEM CALCULATION

### FEM analysis of the bending tests

The analysis of the coupons was done with ANSYS (Ansys Inc., USA) using the dedicated package for composites (ACP). This module allows for a flexible definition of typical composite fabrics and laminates. The software allows for using 3-dimensional elements, which is critical in the case of our stacks of uni-directional plies when loads appear in the thickness direction. The software also allows for solid modelling of the metal-composite interaction as in the case of a four-point test bench in a single step.

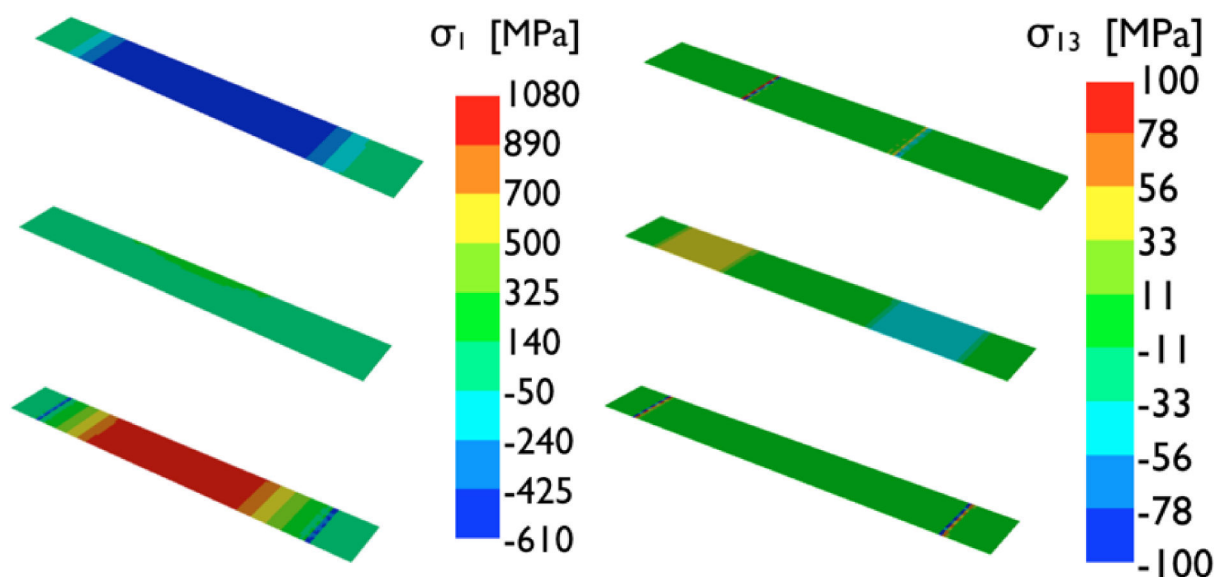


Fig. 3 - FEM evaluation of the stress distribution in a colour scale of three plies (top, middle, bottom) of the coupon's stack. Left panel: longitudinal stress  $\sigma_1$  (positive for tension, negative for compression; units are MPa). In the top ply the maximum stress happen in between the two loading rollers, with a constant value in between, as expected from elastic theory. In the bottom ply the position of the loading rollers are clearly seen as stress concentration lines. Right panel: shear stress  $\sigma_{13}$  (units are MPa). These stresses correspond to the shear loads that can cut the planes of the composite transversally to the fibres, in the thickness direction. See text for details.

In Fig.2 we show the result of the calculation (solid line) of load vs. displacement. The calculation, not being an explicit FEM calculation, is just truncated at some value. Up to 1.4 mm displacement, the agreement is well within the experimental spread (10%). In the following range up to 2 mm (the point we observed as failure), the calculation provides loads below the measured values (within 15%) for any given displacement. Therefore our FEM calculation represents fairly well the bending results, with an uncertainty from 10 to 15 %, depending on the range of load and/or displacement.

The model systematically provides load values below the measured ones in the upper 30 % of the range, before failure. Using the failure reference value of 2 mm displacement, the model provides a conservative value of load for future evaluations of plate designs.

### Stress Distribution

The FEM calculation allows for a detailed description of the stresses happening in the coupons at any step of load and deformation. In Fig.3 (left panel) we show the stress distribution, in color scale, of the longitudinal component  $\sigma_1$  (positive for tension, negative for compression), corresponding to three plies placed at the top, middle and bottom positions of the stack (thickness direction). The stress values correspond to the load in which the (mid-span) deflection is 2 mm, which is the value we have measured as point of the initial failure. The compression dominates the region in between the loading rollers of the test-bench in the ply on the top. In the opposite ply, at the bottom, it is the tensile stress wich dominates in between the rods. The stress values, and type, changes smoothly in the transition from ply to ply of the stack. Only residual stresses happen in the tails of any ply, beyond the rollers. In the top and bottom plies, the position of the rollers of the test bench are clearly seen as stress concentration transverse lines, due namely to friction.



The shear stress  $\sigma_{13}$  is plotted in Fig.3 (right panel), also for the three plies described before. The values are relatively low compared to the shear strengths but for the central plies just in between the loading rollers of each side (cf. with Fig.1, left panel). These stresses correspond to the shear loads that can cut the planes of the composite transversally to the CF fibres, in the thickness direction.

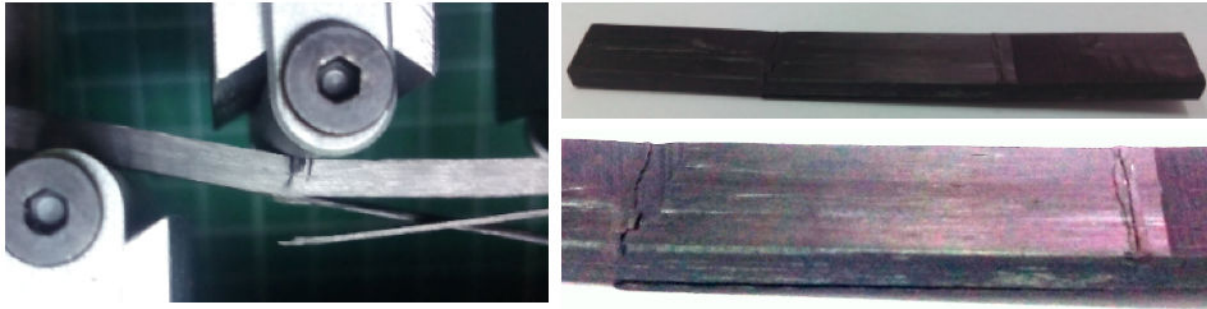


Fig. 4 - Pictures of one of the coupons during and after the bending test. Left: the coupon under a load that has caused the breaking and of delamination of some plies of the stack. Right: one coupon after the bending test. The transverse cracks under the loading rollers are clearly visible. See text for details.

## FAILURE

The failure models of laminate composites describe failure in a two-step process. The initial step, or first failure, happens locally and is typically described according the stress state in one lamina. It is due to fibre breaking or matrix cracking (the delamination of layers is more related to manufacturing anomalies). There are several criteria defined according if they combine (interacting) or not (no-interacting) the strain and stress components in mathematical formulations, to be compared to material strengths.

We used the Tsai-Hill model, a quadratic formulation that is proved to provide reliable results (Athanasios, 2012), providing that accurate composite strengths are known (Sun, 1996), and using a 3-dimensional analysis. The main drawback of this criterion is the non-differentiation of tensile and compressive stresses.

In a second step, if the composite strengths were exceeded, a propagation model would modify the properties of the corresponding layer. This degradation process would cause breaking after accumulation of local failures. Note, however, that the FEM model we are interested in is not dedicated to the study of the failure itself. Therefore the model does not need to include scratch creation or further propagation of the first failure. We obtain an evaluation of how stresses and strains evolve and, eventually, reach a first-failure critical value. This analysis is more than adequate for the discussion. It allows for an effective and robust insight into the problem, while avoiding further modelling of aspects that are beyond the scope of this work. Using our FEM model, we can obtain the corresponding safety-factor at any stage of the applied load and evaluate the possible failure status.

In Fig.4 we see a photo of one of the coupons during and after a bending test. The macroscopic cracks were always initiated in the line below the loading rollers; and propagated through the stack. The shear stresses next to the bottom plies make that those plies set free from the stack, also pulled by tension strains. In the Fig.4 some loose packs of strands are clearly visible. The observed de-lamination failure happens due to propagation processes.



Further studies to refine the value of displacement to the origin of cracks (for instance, based in a high-speed imaging) would poorly help to better define the limit loads, considering the spread observed in the measurement of different coupons. This is way considering a 2 mm displacement as reference value for the definition of failure stress distributions, and not paying attention to the span of that value within  $\pm 0.25$  mm (8%), makes sense in our discussion.

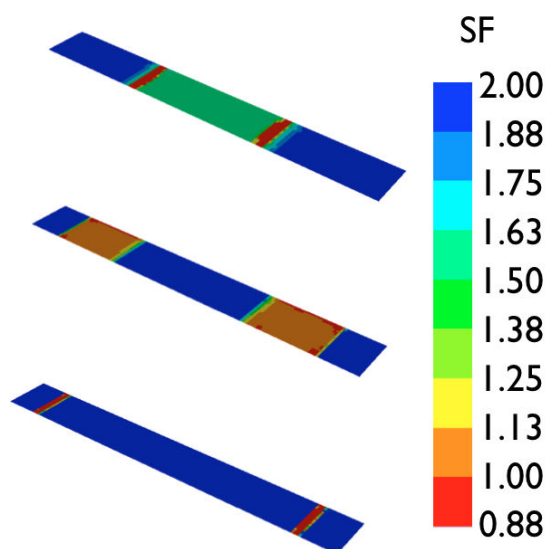


Fig. 5 - FEM evaluation of the security factor distribution of three plies (top, middle, bottom) of the stack making the coupons. The factor has been calculated according to the Tsai-Hill criteria for first failure. The values, in colour scale, correspond to the stresses evaluated at 2 mm (mid-span) displacement of a four-point bending test. In the top and bottom plies, about the position of the rods of the test bench, the material has clearly overpassed the critical value. In the intermediate plies, the distribution goes close to critical values in wide areas in between the loading rollers. See text for details.

The data show clear failure at a displacement value of 2 mm. We can examine the stress and strain distributions of the plates at that point, provided by the calculations. Although it is the safety factor (SF) value defined by the (first) failure criterion that gives the straight information about the state of the coupon. In Fig.5 we plot, in colour scale, the SF defined by Tsai-Hill criterion for our model, applied to a bending test of the coupons. The values are plot again for three plies of the stack at the top, middle and bottom positions, corresponding to a (mid-span) displacement of 2 mm. The results show that under the loading rollers of the top and bottom plies, the SF distribution is below the critical unitary value. Also the SF distribution in the intermediate plies goes towards the limit value in the region in between the rollers. The tensile and shear loads in the bottom plies pull away the sides of the crack. It does not happen in the top plies, with compressive loads. The propagation may cause the further de-lamination of some plies, as in the coupon of Fig.4.

The FEM model shows the first-failure condition consistently happening at the value we have observed failure in the bending test, cf. Fig.2. This analysis provides us with an operational procedure to define failure, by looking to the weaker region, and disregarding propagation modes.

Considering the purpose of our work, based in the use of a commercial material and software, it would be hardly worth, at this stage, to dig neither into the distinctions about matrix or fibre failure, nor the accuracy of the strengths used as reference. Indeed, the interacting criteria are known for not providing clear insight in the basic processes causing failure, due to their own mixed formulations.

## PLATE RIGIDITY STUDIES

The interest in having a validated model is to evaluate the design of bone plates for future use for in-vivo tests. The standards ASTM F382 and ISO 9585 describe the bending test procedures and results related to bone plates, namely the bending stiffness and strength. Actually the standards refer to metallic plates, considering the specific characteristics of bone plates: the holes and possible (transverse) curvature. The four-point test is mandatory, and there are recommendations about the setup of the plates in between the loading rollers related to the position of the holes, distances relative to the size of the plate, and roller diameter ranges, and its ratio to hole inter-space.

In order to make a general comparison, we calculated the bending stiffness following F382 as a function of the thickness of the plate. We used as reference a plate of rectangular cross section, 12 mm width, 130 mm length, rather close to commercial models, and no curvature. In Fig.6 we plot the stiffness obtained from calculations done with different thicknesses ranging from 1 to 6 mm (a commercial plate of this size would have 4.5 mm). The results correspond to stainless steel 316-L (triangles), and the CFR-PEEK we analysed in our study (squares). The stiffness of CFR-PEEK is always greater, ranging from a relative difference of 38% (2 mm) to 46% (6 mm), compared to 316-L. If simple straight holes were introduced (seven holes, for this size of plate), the stiffness values for CFR-PEEK, would decrease by 29 % in respect to a solid plate (stars).

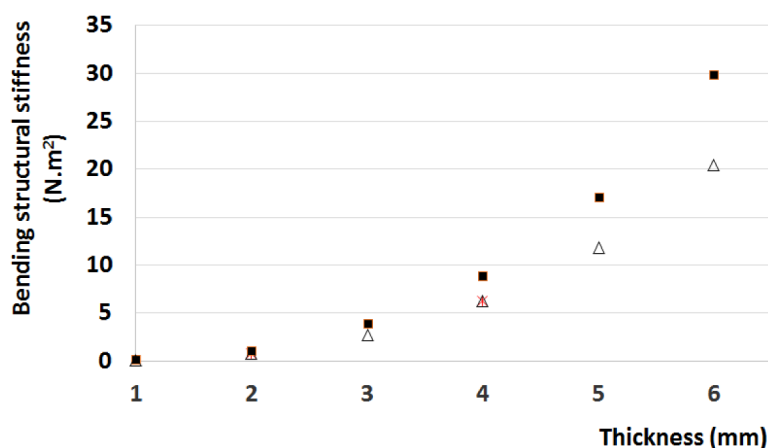


Fig. 6 - Calculated bending rigidity as a function of the thickness of a reference flat plate, with rectangular section, 12 mm width, 130 mm length. The results are for stainless steel 316-L (triangles) and the CFR-PEEK plates used in this work (squares). The introduction of holes in the CFR-PEEK plates produces a reduction in stiffness of about 29% relative to solid plates (stars, entangled with the symbol for 316-L). See text for details.

The higher stiffness of the CFR-PEEK plates, for the same thickness, results from the high content of fibre of the pre-preg we are using, which makes a difference in respect to other studies (Fujihara, 2003). We have a two-fold result. We can tune the rigidity in steps by modifying the number of layers of our stack of composite, in a rather smooth and under-control way. Secondly, we aim to use our plates with small size animals (rabbits). Therefore we need to get a plate as thin as possible to avoid troubles in surgery procedures. With our results, it seems clear that we can reduce the thickness in an important factor to obtain a plate of variable rigidity compared to metals.

## CONCLUSIONS AND OUTLOOK

We have prepared a study of CFR-PEEK plates using FEM and based in material properties either provided or derived from composite micromechanics models. We also prepared

coupons to measure in a bench dedicated to four-point bending tests. The comparison of the measured results and the model was proved satisfactory. Although the full description of the failure is missing in the model, the key information related to our study is properly provided. We can trace the failure status found to the SF distributions, irrespective of the failure description itself.

The purpose of testing the calculation model is to proceed to analyse the design of CFR-PEEK plates dedicated to in-vivo tests of bone reduction with rabbits. The base of the effort is triggered by the new pre-pregs available in the market that can make efficient the production of this type of plates, avoiding complex production procedures.

In our study, bending and stiffness were measured in a single cycle test. In the development of the project, the next step is to investigate both an optimized plate design and their fatigue performance. The description of fatigue behaviour of CFR-PEEK is rather complex and the results related to bone plates, always functional, are very scarce (Brown, 1990) (Steinberg, 2013). The results confirm the endurance of the CFR-PEEK, for both plates and screws (Tognini, 1999). We want to study the fatigue for the material processed from pre-pregs. The design we pursue has to follow the rigidity needs of the bone healing, including the whole system of bone, plate and screws, as demonstrated by (Gautier, 2000) (Huang, 2005). We have now a validated model to evaluate the design and making oriented choices for further production and testing.

After the satisfactory results we have found, we believe that there is a new opportunity to dig into the possibilities of deployment of CFR-PEEK for bone plates as an alternative to metal plates.

## ACKNOWLEDGMENTS

This work was supported by grant EM 2012/140 (Xunta de Galicia, Spain).

## REFERENCES

- [1]-Ali M.S., French T.A., Hastings G.W., Rae T., Rushton N., Ross E.R.S., Wynn-Jones C.H., Carbon fibre composite bone plates development, evaluation and early clinical experience, *J. Bone Joint Surg. [Br]*, 1990, 72-B, p. 586-91.
- [2]-Athanasios J. K., Stefano Proia, Evaluation of the Reliability Performance of Failure Criteria for Composite Structures, *World Journal of Mechanics*, 2012, 2, p.162-170.
- [3]-de Baere I., Van Paepegem W., Degrieck J., Comparison of different setups for fatigue testing of thin composite laminates in bending, *International Journal of Fatigue* 31, 2009 p.1095-01
- [4]-Brown S.A., Hastings R.S., Mason J.J., Moet A., Characterization of short-fibre reinforced thermoplastics for fracture fixation devices, *Biomaterials* 11, 1990 p. 541-547.
- [5]-Chamis C.C., Simplified Composite Micromechanics Equations for Hygral, Thermal and Mechanical Properties, NASA Technical Memorandum 83320, 1983.
- [6]-Chamis C.C., Simplified Composite Micromechanics Equations for Strength, Fracture Toughness, Impact Resistance and Environmental Effects, NASA Technical Memorandum 83696, 1984.

- [7]-Cordey J., Perren S.M., Steinemann S.G., Stress protection due to plates: Myth or reality? A parametric analysis made using the composite beam theory, *Injury, International Journal of Care Injured*, 31, 2000, S-C, p.1-13.
- [8]-Fujihara K., Huang Z.M., Ramakrishna S., Satknanantham K., Hamada H., Feasibility of knitted carbon/PEEK composites for orthopaedic bone plates, *Biomaterials*, 2004, 25 (17), p.3877–3885.
- [9]-Fujihara K., Huang Z.M., Ramakrishna S., Satknanantham K., Hamada H., Performance study of braided carbon/PEEK composite compression bone plates, *Biomaterials*, 2003 24 (15), p.2661–2667.
- [10]-Gautier E., Perren S.M., Cordey J., Effect of plate position relative to bending direction on the rigidity of a plate osteosynthesis. A theoretical analysis, *Injury, International Journal of Care Injured* 31, 2000, S-C, p.14-20
- [11]-Gilliot A., From carbon fibre to carbon-fibre-reinforced thermoplastics, *JEC Composites Magazine*, 71, 2012, p.60-62.
- [12]-Hopkins, D.A. and Chamis, C.C., A unique Set of Micromechanics Equations for High Temperature Metal Matrix Composites, *NASA Technical Memorandum* 87154, 1985.
- [13]-Huang Z.-M., Zhang Y., Ramakrishna S., Modelling of the progressive failure behaviour of multilayer knitted fabric-reinforced composite laminates, *Compos. Sci. Technol.* 2001, 61(14) p.2033–46.
- [14]-Huang Z., Fujihara K., Stiffness and strength design of composite bone plates. *Composites Science and Technology*, 2005, 65, p.73–85.
- [15]-Kurtz S. M. , Devine J. N., PEEK Biomaterials in Trauma, Orthopedic, and Spinal Implants, *Biomaterials*, 2007 November; 28 (32), p. 4845–4869.
- [16]-Miyagawa H. at al., Comparison of experimental and theoretical transverse elastic modulus of carbon fibers, *Carbon* 44, 2006, p. 2002–2008.
- [17]-Scholz M. S., The use of composite materials in modern orthopaedic medicine and prosthetic devices: A review, *Composites Science and Technology* 71, 2011, 1791–1803, doi:10.1016/j.compscitech.2011.08.017
- [18]-Steinberg L., Rath E., Shlaifer A., Chechik O., Maman E., Salai M., Carbon fiber reinforced PEEK Optima — A composite material biomechanical properties and wear/debris characteristics of CF-PEEK composites for orthopedic trauma implants, *Journal of the Mechanicla behaviour of biomedical materials*, 17, 2013, p. 221-228
- [19]-Sun C.T., Quinn B.J., Tao J., Oplinger D.W., Comparative evaluation of failure analysis methods for composite laminates, 1996, report DOT/FAA/AR-95/109
- [20]-Tayton K., Johnson-Nurse C. , McKibbin B., Bradley J., Hastings G., The use of semi-rigid carbon-fibre-reinforced plastic plates for fixation of human fractures: results of preliminary trials. *J. Bone Joint. Surg. [Br]*, 1982, 64-B, p.105-11.
- [21]-Tognini R., Loher U., Peter Th., Raschle R., Mayer J., Wintermantel E., Fatigue properties of cf/peek cortical bone screws produced by composite transfer squeeze forming, *Proceedings of the ICCM -12 Conference*, Paris, 1999.